

Pressure impact on physical behavior of intermetallics

Habilitation thesis

Jiří Prchal

Department of Condensed Matter Physics

Charles University, Faculty of Mathematics and Physics

Prague 2021



Preface:

The present work brings a selection of intermetallic compounds studied by means of external mechanical pressure and consequent influence on their structural and electronic properties. Besides temperature and magnetic field the pressure, as the most pure way of the crystal lattice changes, represents the least utilized method for changing the physical variable due its technical difficultness. It is also the reason for sometimes longer way needed between the studied system discovery and the adequate high pressure data acquisition. The present stage of mastering of the high-pressure techniques nevertheless enables the first pressure experiments to be managed already by students. In numerous cases, the attached publications contain results obtained by students of all university levels (PhD, MSc, Bc) under my leadership.

The particular publications, even the daily work and especially the final formation of this commented overview would be hardly possible without support and encouragement of majority of my colleagues in the Department of Condensed Matter Physics, namely prof. Pavel Javorský, doc. Ladislav Havela, doc. Martin Diviš, dr. Jan Prokleška, dr. Jaroslav Valenta, prof. Vladimír Sechovský and many others, as well as colleagues and friends from the high-pressure group in the Institute of Physics of the Academy of Sciences, dr. Jiří Kaštil, dr. Martin Míšek. Besides colleagues from Prague my special gratitude belongs to my “japanese supervisor” prof. Hideaki Kitazawa and also to dr. Takashi Naka who opened the fascinating field of high pressure problematics to me, as well as to dr. Jean-Christophe Griveau for his unlimited patience during teaching me the techniques of Bridgman-anvil pressure cells preparation. It is impossible to personally include names of all supporting colleagues to whom belong my great thanks. As well as it is impossible to express the real level of thanks to my wife Markéta for her every-day patience and silent support of my scientific activities.

Content:

Pressure as a unique tool for characterization of materials	2
High pressure techniques	3
Summary of published results – comments on attached publications	
<i>A: Structural changes in magnetic materials under pressure</i>	7
<i>B: Magnetism in rare-earth based RT_2X_2 tetragonal compounds influenced by pressure</i> ...	11
<i>C: Pari-magnetism in RCo_2 under pressure</i>	13
<i>D: Pressure impact on properties in U and Ce-based compounds</i>	16
References	22
List of attached publications (including declaration about author contribution)	24



Pressure as a unique tool for characterization of materials

Physical properties of materials are thoroughly investigated by myriads of experimental methods and theoretical approaches. In many experiments a material is exposed to a small probing stimulus and its response is recorded. For example, weak magnetic fields inducing magnetization of different sign tell us whether materials is a paramagnet or diamagnet. However, external actions can be taken to change the material under study. One can thus probe the environment of an equilibrium state or the stability of thermodynamic phases in different situations. Exposing a material to so called extreme conditions, a strongly non-linear behavior can be observed. One can meet an instability of the actual phase and a phase transition. Definition and theory of phase transitions is described in numerous textbooks (e.g. in [1,2]).

In the solid state science the most general thermodynamic variables to tune the studied material are temperature, magnetic field, or external pressure. Changing these physical conditions are subject of specific approaches and specialized branches of science.

In particular - Temperature as a parameter is a subject and main tool for (extremely) low-temperature physics.

Magnetic field - A development of high-magnetic field magnets supports the availability of strong external fields. Namely the discovery of superconductivity has initiated these efforts and the equipment containing strong magnets based on a superconducting materials providing magnetic fields of several tens of Tesla are commercially available nowadays.

Pressure - The least utilized thermodynamic variable from the above-mentioned ones is pressure, mainly for its technical difficulty, although last decades evidenced substantial development of the high pressure cells and devices, namely after Percy Bridgman introduced his opposite-anvils setup. This development of pressure cells and progress in high pressure techniques supported by the progress in technologies in general, enabled the boost of materials science and even discoveries of new emergent phenomena in the particular fields of science.

One may compare the effect of external pressure on the matter with other used physical variables on the energy scale in the following way. Suggesting application of 1 GPa on the piece of an iron sample counting N_A atoms one can obtain an elastic energy of ≈ 0.9 meV / atom (for BCC structure with $a = 287$ pm, using the value of bulk modulus of iron at room temperature $B_{Fe} \approx 170$ GPa). Similar level of energy effort corresponds to change of temperature by ≈ 20 K. On the scale of magnetic field applied on a single spin (with magnetic moment $\mu = 1 \mu_B$) such energy corresponds to ≈ 15 T.

Thermodynamic description of pressure is based on the principal definition $p = F/A$. Here p is pressure, F the force acting on the surface with the area A . Effect of the pressure on the matter can be imagined as a force acting on an elementary surface area of an infinitesimal cube in direction



parallel to the surface area normal in every point. Due to the fact of the force being a vector, the resulting tension (supposing equilibrium state) is thus considered as a tensor, generally appearing as

$$\sigma_{ij} = \begin{pmatrix} \sigma_{xx} & \sigma_{xy} & \sigma_{xz} \\ \sigma_{yx} & \sigma_{yy} & \sigma_{yz} \\ \sigma_{zx} & \sigma_{zy} & \sigma_{zz} \end{pmatrix} \quad (1)$$

Here, the diagonal elements σ_{ii} represent normal action, perpendicular to the surface of the pressurized elementary cube, whereas the off-diagonal elements $\sigma_{ij, i \neq j}$ are responsible for the tangential forces, i.e. the shear stress. In the special case of no shear stress and if the diagonal elements are equal, we speak about the hydrostatic pressure. Uniaxial pressure is present if only one diagonal element has a non-zero value.

High pressure techniques

When characterizing the studied material by standard – or even less standard – methods one has to master the corresponding set of experimental approaches and use of the appropriate equipment. When the enhanced pressure is used, another specific approach has to be taken into account. First one has to use the appropriate pressure cell in order to apply the pressure required. Second, it is the mastering of the setup of the desired type of measurement for determination of the corresponding physical property, while the sample is placed inside a very restricted space. The experimental methods with focus for use in conjunction with high pressures are described in numerous textbooks – e.g. [3-5].

The variety of high-pressure techniques is very large due to numerous scientific fields dealing with changes of the studied subject upon elevated pressures. Those are for example:

- * Geophysics (with interest in enormous pressures in combination with enhanced temperatures for simulation of effects and conditions present in the deep levels and core of the Earth and other planets' cores);
- * Food and bio sciences (dealing with pressure effects on living organisms and their ability to survive when exposed to high pressure, which is used in food conservation by pressure application; there are also medical applications based on for example pressure-induced deactivation of tumors and cancer cell lines);
- * High-pressure chemistry (focusing on pressure as a parameter that enables chemical reactions and chemical bonds changes, often enables synthesis of new materials or their structural and chemical variants that could never appear otherwise);
- * Solid-state physics (phenomena like structural transitions, pressure induced superconductivity, quantum phenomena).

As our field of interest is the branch of solid state physics, we will introduce the pressure cells usually involved in experimental solid-state physics. It is interesting that various high-pressure laboratories



developed different types of cells for similar types of measurements. This fact reflects the extended know-how required for successful high pressure research. The multitude of procedures and practical tricks is in reality difficult to share between laboratories, hence individual schools have naturally developed. The pressure cells differ by **i)** requested pressure range and **ii)** type of physical property to be explored.

Choosing a proper type of cell one has to be aware of particular advantages, which are, however, always accompanied by certain limitations. A typical example of such situation is a smaller sample space available in case of higher pressure range of the cell. Another typical problem, which the pressure scientists need to deal with, is the worse hydrostaticity at higher pressures caused by solidification of the (originally liquid) pressure transmitting media. Therefore there is an ongoing activity aiming at improvement of pressure transmitting media, which are responsible for equal redistribution of the pressure within the sample space – i.e. hydrostatic conditions acting on the studied sample. Searching for an appropriate medium to be used in the sample space is a problem since the beginning of the high pressure research as such. Among others the media like industrial oils, braking fluids, fluorinerts, or alcohol-mixtures (e.g. methanol-ethanol) are routinely used for their specific properties. Together with development of new pressure cell types able to reach higher pressures many of these liquids freeze upon increased pressure, resulting in degradation of hydrostatic conditions if the pressure medium solidifies. Consequently, a new liquid media are sought in order to enhance the pressure range of the liquid state.

An example of a specially developed media for pressure experiments and its improvements is series of Daphne Oils by group of prof. Murata and Idemitsu Kosan Co., Ltd. company [6-8]. The first developed one – Daphne Oil 7373 – which is liquid up to $p^{\text{sol},7373} = 2.2$ GPa at room temperature. Upon cooling down it solidifies at $T^{\text{sol},7373} = 180$ K at ambient pressure [6]. These limits shift significantly for the newer version of Daphne Oil 7474, which solidifies at $p^{\text{sol},7474} = 3.7$ GPa at room temperature [7] or $T^{\text{sol},7474} = 150$ K at ambient pressure (**T1**). This improvement enables to cover the whole pressure range of the most often used pressure cells in DCMP (see below) by hydrostatic conditions.

The newest Daphne Oil 7575, available since 2016, was characterized within a student project at Charles University, FMP, the data reported in the attached paper **T1** are the first characterization report of this high-pressure liquid pressure medium upon cooling down. Daphne 7575 is actually innovative in a bit broader pressure range of the liquid state compared to Daphne 7474 – it has the point of

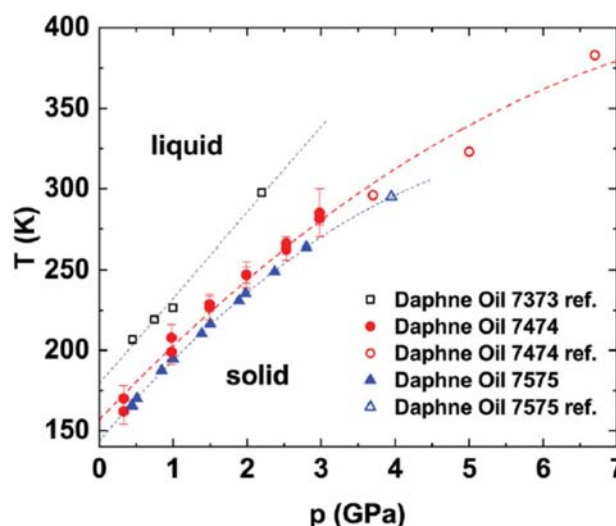


Fig.T1: The solid-liquid phase boundary for three existing Daphne Oils. The empty symbols stand for previously reported data on Daphne Oil 7373 [6], Daphne Oil 7474 [7] and Daphne Oil 7575 [9]. Figure taken from T1.



solidification $p^{\text{sol},7575} = (3.9-4.0)$ GPa at room temperature [9]. The pressure development of freezing temperature $T^{\text{sol},7575}$ was followed in the low-temperature experiment resulting in estimate of the solid-liquid boundary as shown in Fig. T1. Another more practical advantage is easier distribution of this medium outside the country of origin (Japan) contrary to Daphne 7474, which is practically unavailable outside Japan due to strict export regulation. Aside of the pressure dependence of the freezing temperature of Daphne 7575 (first published report), Daphne 7474 and Daphne 7373, also other properties were characterized and described in **T1** including compressibility, pressure decrease upon cooling or hydrostaticity over the whole studied pressure range up to 3 GPa.

Besides Daphne Oils many other pressure exchange media used in pressure experiments can be used – in all states and forms – gases, liquids, and solid ones, as well. In most of our pressure experiments with liquid pressure transmitting media we have used one of the available Daphne Oils. Spindle oil OL-3 or a steatite (solid) served as a pressure transmitting medium in another few cases.

Pressure cells used to obtain data in the attached publications:

The pressure cells used in our laboratory and namely the cells which were used to acquire results presented in the following list of publications are summarized here:

• **Piston-cylinder clamp pressure cell (1 GPa)**

Material: CuBe (single layer)

Pressure range: up to 1 GPa nominally

Available types of physical properties to be measured: Electrical resistance, dilatometry using strain-gages



Applicable in connection with Closed-cycle cryocooler (CCR; Sumitomo Heavy Industries / Janis Research)

Pressure determination: pressure dependence of resistance of the manganin wire (at RT)

Pressure transmitting medium: Spindle Oil OL-3, Daphne Oil 7373

Used to obtain data in presented publications: A2,A3

• **Piston-cylinder clamp pressure cell (1 GPa)**

Material: CuBe (single layer)

Pressure range: up to 1 GPa nominally

Available types of physical properties to be measured: Magnetization, magnetic susceptibility

Applicable in connection with MPMS device (Quantum Design)

Pressure determination: Superconducting transition of lead - determined at low temperatures





Pressure transmitting medium: Spindle Oil OL-3, Daphne Oil 7373

Used to obtain data in presented publications: B1,B2



Material: CuBe (outer layer)
+ NiCrAl (inner cylinder)
– i.e. double layer cell

Pressure range: up to 3 GPa nominally
(3.2-3.4 GPa reached in some cases)

Available types of physical properties to be measured: Electrical resistance, AC-magnetic susceptibility, dilatometry (strain gages), heat capacity (AC-calorimetric method, not used in attached publication, but available as well)

Applicable in connection with all equipment in the laboratories of DCMP and MGML - PPMS (Quantum Design), CCR, 9T cryomagnet with dilution stick (DR), 20T cryomagnet

Pressure determination: pressure dependence of resistance of the manganin wire (room T)

Pressure transmitting medium: Daphne Oils 7373, 7474, 7575

Used to obtain data in presented publications:

T1,A4,A5,A6,B3,B4,C1,C2,C3,C4,C5,D2,D3,D4,D5,D6



Material: body - CuBe,
anvils - WC,
alternatively sintered diamond (PkDia)

Pressure range: up to 12 or 20 GPa –
depending on the variant/size of the anvil-
top and pressure space diameter

Available types of physical properties
to be measured: Electrical resistance

Applicable in connection with CCR, DR

Pressure determination: Superconducting transition of lead - determined at low temperatures

Pressure transmitting medium: steatite (solid)

Used to obtain data in presented publications: D1



Summary of published results – comments on attached publications

A: Structure changes in magnetic materials under pressure

An unexpected structural discontinuity has been observed on numerous compounds among the ternary rare-earth compounds crystallizing in a hexagonal crystal structure (group No.189). A sudden step was observed in temperature and composition evolution of the hexagonal lattice parameters a and c and their ratio c/a , while the volume is preserved at the point of transition – e.g. TbNiAl, TbPdAl, GdNiAl, GdPdAl, $RNi_{1-x}Cu_xAl$ ($R=Tb,Er,Dy$) [10-13], all adopting the mentioned ZrNiAl structure type. On the Fig. A1 one can see the step-like evolution of the lattice parameters for several compounds or series of compounds.

Such effect is difficult to classify within the Landau theory of phase transitions due to the fact that a state parameter is a unit-cell volume but not a lattice constant itself. In correspondence with this fact we estimated that the specific heat measurements in the vicinity of the transformation does not show any anomaly (A1) concluding on the basis of thermodynamics that the related change in

the enthalpy of the transformation is just at the border of detectability using the relaxation method. The consequence is inability of reaching a specific values of the c/a ratio, dividing the states of the crystal lattice to states “above the forbidden c/a ” and “below the forbidden c/a ”. A systematic boundary between these two states could be found among the $RNi_{1-x}Cu_xAl$ compounds as displayed in Fig. A2. Existence of such a gap in c/a values has been confirmed by *ab-initio* calculations which found existence of two independent energy minima in the field of a - c values close to the empirically found ones (A1). Importance of such effect dwells in mechanical properties of the compounds exhibiting a - and c -values in the vicinity of the “forbidden” values. As the c/a gap appears not only in variations of lattice parameters across a series of compounds but also in individual compounds for which the gap area is entered during cooling as a thermal expansion effect, the mechanical strains detach the sample from the sample holder at the structure transformation (Fig. A3). This

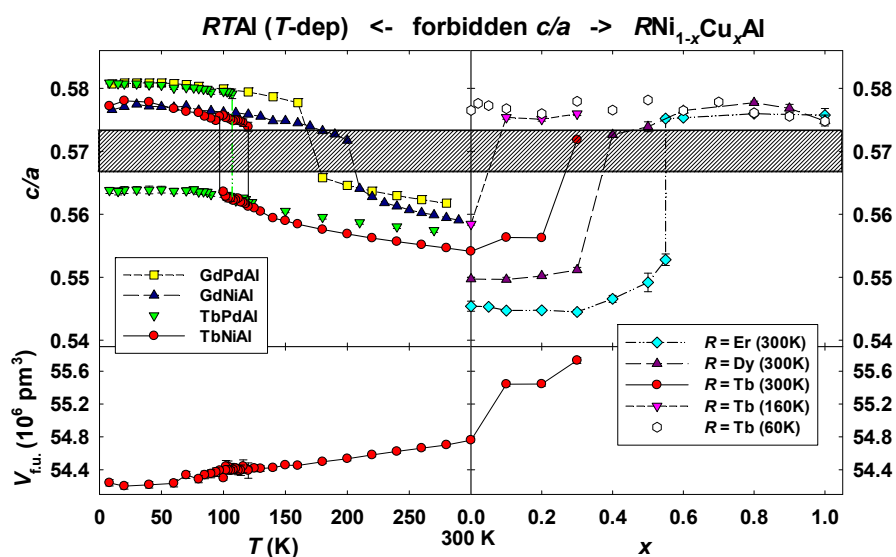


Fig. A1: The discontinuity in the evolution of lattice parameters a, c of the compounds adopting the ZrNiAl-type crystal structure type observed directly by X-ray diffraction on the temperature- and composition development of the lattice. The hatched area depicts the empirically estimated interval of the forbidden c/a values. Figure taken from A1.



simple issue stands behind the fact that there are only very few data of specific heat of these compounds presented in literature. In the case of a single crystal (TbNiAl) we experienced even loss of mechanical integrity and fragmentation of the sample into more pieces when cooling down.

Having determined the evolution of the structure discontinuity with temperature and composition, we were interested in its presence and development upon application of external pressure. A high-pressure XRD experiment at low temperatures as a direct estimation of lattice parameters needs to use a synchrotron facility. Another and more accessible option is provided by impact of the structure anomaly on electrical resistivity [12]. In this case the sample quality deterioration causes the resistance increase at the point of the structural transformation and thus reflects the presence of the structure step-like change.

Inspired by this fact we measured electrical resistance of TbNiAl and GdNiAl upon pressure application and estimated a clear pressure-driven variations of the structure gap boundary (A2,A3) with evident preference of the structure with a lower c/a ratio in both cases (Fig. A4).

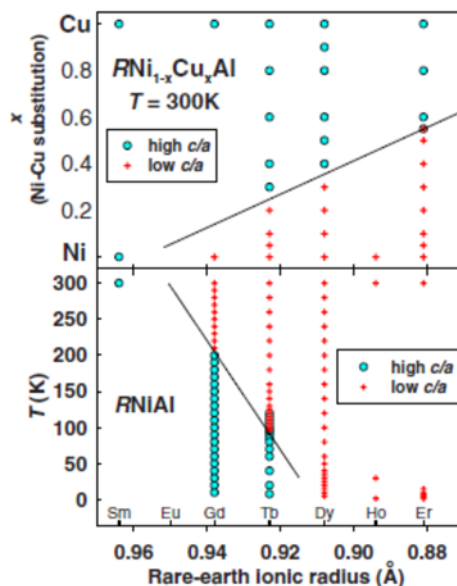


Fig. A2: Systematic evolution of the boundary between a high c/a and a low c/a ratio within the $RNi_{1-x}Cu_xAl$. Figure taken from A1.

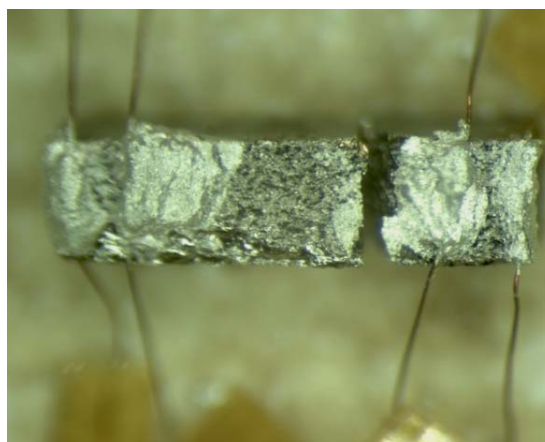
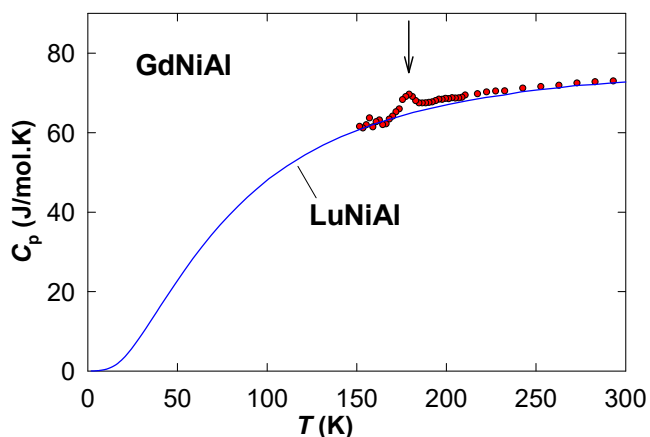


Fig. A3: Structure discontinuity on the studied $RNiAl$ samples resulting in technical issues. Left – the sample of GdNiAl with temperature of the structural transformation $T_{str} = 180$ K being detached from the sample holder shortly below this temperature during the specific-heat experiment. Similar issue was met for TbNiAl around 110 K. This effect prevented specific heat measurement by a standard relaxation method. Right – the signal of the TbNiAl single crystal used for the electrical resistivity experiment was lost after cooling down to 100 K. The reason was the broken sample. Figures taken from A1 and A2.

Stabilization of the low c/a phase is in agreement with a weaker interplanar bonding between the layers in the hexagonal ZrNiAl-type structure and corresponds to the estimated linear compressibility being more than twice higher along the c -axis in TbNiAl comparing to the a -axis [14].

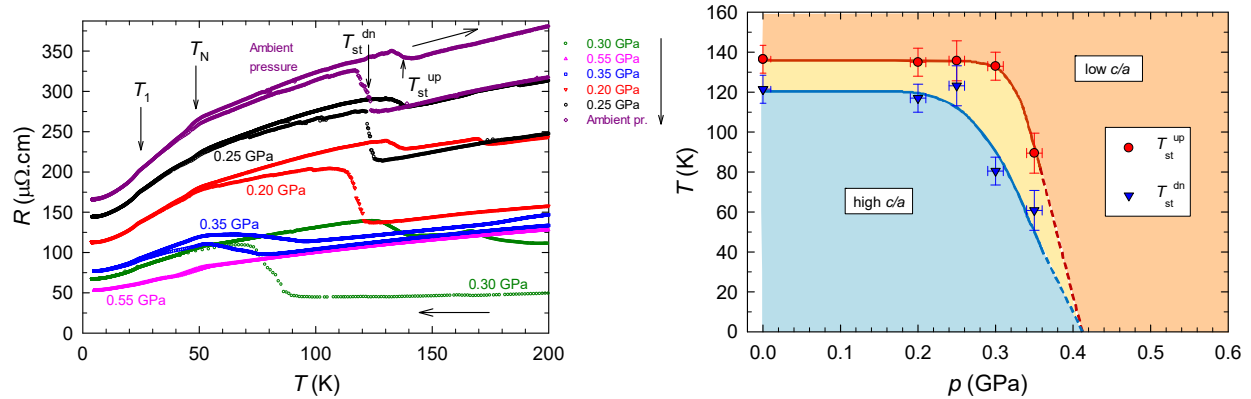


Fig. A4: Estimated gap boundary between the low- c/a and high- c/a states in TbNiAl under hydrostatic pressure by utilization of the resistance measurement (left part). Although the sample exhibits a sudden irreversible resistance increase at the point of the structural transformation, the sample did not break like in the case of the measurement under ambient pressure, apparently due to the mechanical support of the sample inside the pressure space. Resulting phase diagram is depicted on the right panel. Figures taken from **A3**.

Besides the pressure-driven evolution of the structure discontinuity, the application of external pressure has impact on magnetic properties, as well. TbNiAl is an antiferromagnet (AF) below $T_N = 45$ K and undergoes an additional magnetic phase transition to another AF phase at $T_1 = 23$ K. Application of hydrostatic pressure does not change T_N significantly but the critical magnetic field, producing a metamagnetic transition to ferromagnetic state observed at ambient pressure at $\mu_0 H_{\text{crit}} \cong 0.2$ T, increases up to 1.2 T at the pressure of 2.8 GPa (**A4**). This is a clear evidence of stabilization of the AF phase with enhanced pressure. On the other hand, the uniaxial pressure applied along the c -direction (**A3**) does not influence the $\mu_0 H_{\text{crit}}$ or even reduces it slightly (Fig. A5). Considering the difference in the impact of hydrostatic or uniaxial pressure it is evident that the lattice and relevant ionic distances are affected in different ways. The uniaxial pressure definitely decreases the distances along the c -direction leaving the hexagonal planes unaffected or possibly even a bit expanding. The hydrostatic pressure acts probably also on the c -direction more significantly than on the a -direction (as disclosed by anisotropic compressibility published in [14]). Nevertheless, in the case of the hydrostatic pressure the distances within the basal plane become closer, while the interactions between magnetic ions within the basal plane (the nearest-magnetic-ions) play the decisive role for the magnetic behavior of the whole system.

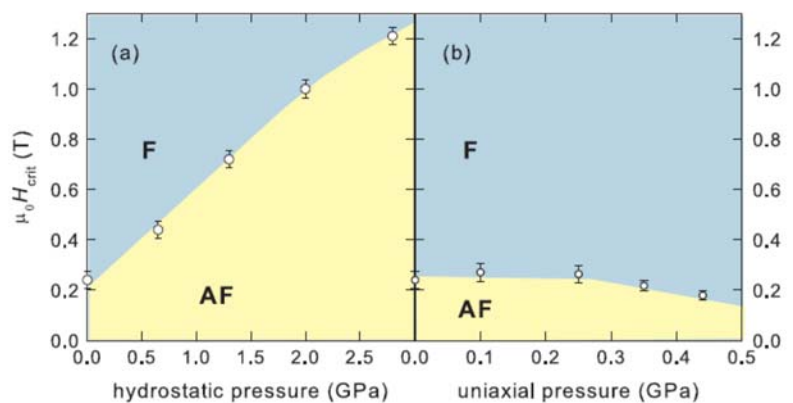


Fig. A5: Magnetic-field - pressure phase diagram of TbNiAl representing the impact of the hydrostatic (a) and the uniaxial pressure (b) on the critical magnetic field necessary for destabilization of the AF phase. Figure taken from **A4**.



Similar method of following the structural transition in the resistivity changes as described above (for TbNiAl and GdNiAl) was used for the study of samples from another family of compounds – the ternary 122 systems, namely CePd₂Al₂ (**A5**) and CePd₂Ga₂ (**A6**). Both compounds crystallize in the tetragonal CaBe₂Ge₂-type crystal structure, in which the compounds are usually unstable and undergo structural transition to another structure type of lower symmetry. Both compounds were studied under application of hydrostatic pressure up to 3 GPa.

Structure transition is observed also in CePd₂Al₂ at the temperature of $T_{str} = 13$ K, below which the crystal structure changes from tetragonal to orthorhombic at ambient pressure. The magnetic properties are characterized by an antiferromagnetic ordering below $T_N = 2.8$ K [15]. The structure changes in CePd₂Al₂ were discussed in the context of so called vibron states – a consequence of electron-phonon interactions [16,17]. The knowledge of crystal-structure transformations is an essential part of this research. The pressure studies revealed an important piece of knowledge. We discovered another low-temperature pressure-induced structural phase at pressures above 0.6 GPa (Fig. A6). The different nature of the two low-temperature structures is evident on the pressure development of the temperature dependence of resistivity (Fig. A7). The resistivity shows a clear decrease with cooling at the temperature of structural phase transition at ambient pressure. This character is changed for pressures above 0.6 GPa signifying transition of a different nature. The resistivity behavior above 0.6 GPa resembles that in CePd₂Ga₂ [18] and thus invokes an idea of similar structural changes.

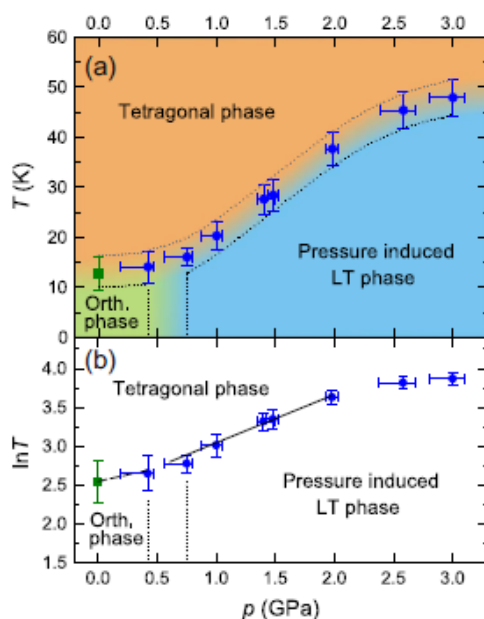


Fig. A6 (left): Temperature-pressure phase diagram of CePd₂Al₂ determined from the data of electrical resistivity (detail in further text). Figure from **A5**.

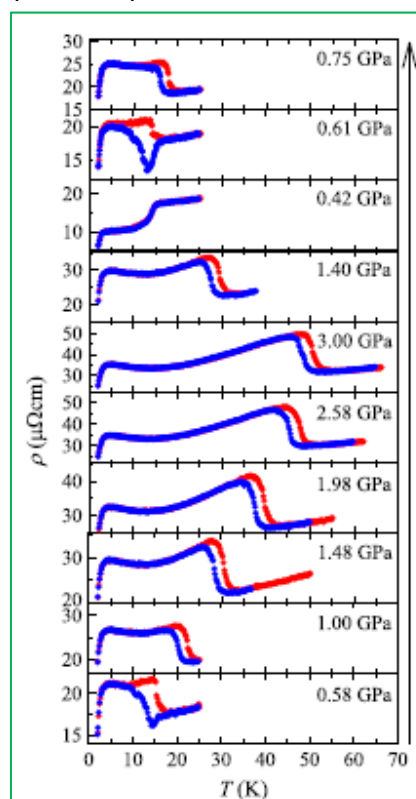


Fig. A7 (right): Temperature dependence of electrical resistivity of CePd₂Al₂ at various pressures. The data are displayed in the order of measured pressure points (marked by an arrow). The cooling (heating) regime is in correspondence with the used blue (red) color. Figure taken from **A5**.



For the CePd_2Ga_2 compound the crystal lattice changes from tetragonal to another structure type at 125 K in ambient pressure (Fig. A8). This structure transition shifts to higher temperatures at elevated pressures and its character remains the same over the whole used range of pressures. Based on recent studies [19], the low-temperature structural phase of CePd_2Ga_2 (and presumably also the low- T pressure-induced one in CePd_2Al_2) was resolved as an orthorhombic structure, space group (SG) No. 67 which is of lower symmetry than the original room-temperature tetragonal (SG No. 129) but higher symmetry than the initially conjectured triclinic model as noted in Fig. A8. In fact, the low-temperature structures in CePd_2Al_2 and CePd_2Ga_2 are of the same type, but differ by size of the orthorhombic distortion of the high-temperature tetragonal structure.

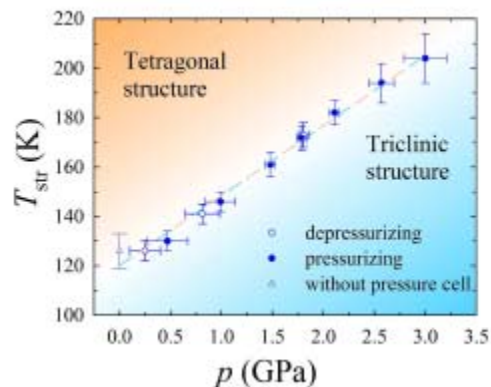


Fig. A8: Temperature-pressure phase diagram of CePd_2Ga_2 determined from the data of electrical resistivity. Figure taken from **A6**. As the structure at low temperatures was not ultimately resolved at the time of publication, the low- T phase is marked as “Triclinic”. Later studies distinguished this phase as orthorhombic structure, SG No. 67 [19].

In the point of transition for both of these compounds the crystal structure changes its symmetry and corresponding change of resistivity is reversible in both CePd_2Al_2 and CePd_2Ga_2 , unlike our previously discussed hexagonal ZrNiAl -type structures, where the symmetry at the transformation is preserved but the resistivity irreversibly increases demonstrating clear degradation of the sample. We should remind that in both mentioned cases the magnetic transition appearing at different (lower) temperatures than the structural ones is of the second order type. The structure changes play an important role especially in crystal field and consequent influence on the magnetic behavior (see e.g. [17]).

B: Magnetism in rare-earth based RT_2X_2 tetragonal compounds influenced by pressure

Another tetragonal compound which, unlike previous Ce-based compounds crystallizes in the ThCr_2Si_2 -type of structure, is PrRu_2Si_2 . This structure type is characteristic by a large magnetocrystalline anisotropy. PrRu_2Si_2 is known to exhibit an extraordinarily large anisotropy field of approx. 400 T [20]. This compound exhibits an antiferromagnetic transition at $T_N = 16$ K to an incommensurate spin wave propagation phase and at $T_C = 14$ K it becomes a uniaxial ferromagnet. The high-pressure study up to 0.9 GPa (**B1, B2**) has shown that the ordering temperature T_N is almost not affected by the pressure whereas the T_C significantly decreases. The critical field of metamagnetic transition in the AF phase increases by a factor of 2 under pressure of 0.8 GPa while the Pr magnetic moments remain unchanged in the paramagnetic state.

The compound YbAu_2Si_2 adopts the ThCr_2Si_2 -type of structure, as well. Ytterbium brings a potential for unusual behavior in numerous intermetallic systems including the change of the valence, non-integer valence or valence fluctuations, identified as a possible origin of



unconventional critical phenomena [21]. As the effective Yb volume is different for the Yb^{2+} or Yb^{3+} valence state, the Yb-based systems are usually very sensitive on application of external pressure. Expectation of unconventional properties and interesting electronic behavior after the pressure application is justified in the Yb compounds. The valence in YbAu_2Si_2 was deduced as intermediate [22]. We have thus performed a low-temperature study of YbAu_2Si_2 (**B3**) including theoretical calculations (DFT) which confirmed the system to be close to magnetic instability with the effective magnetic moment of $\mu_{\text{eff}} = 0.1 \mu_{\text{B}}/\text{f.u.}$ reflecting either a minor tendency to valence fluctuations or a small fraction of Yb atoms with the 3+ valence state existing due to lattice imperfections. The temperature dependence of resistivity was successfully described by the phonon scattering model (Fig. B1). The high-pressure experiment up to 3.2 GPa did not reveal any significant change of this state determining this compound as stable nonmagnetic system with the Yb^{2+} valence state with weak electron-electron correlations in the whole studied pressure range and much higher pressure is needed to change the valence state of Yb in this system.

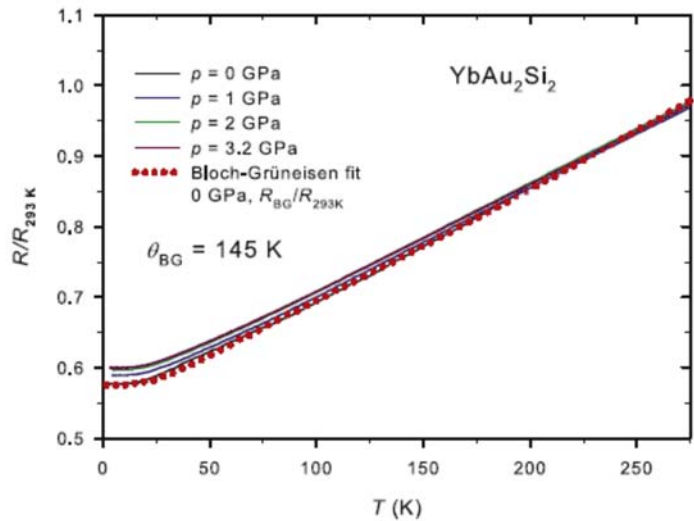


Fig. B1: Temperature dependence of electrical resistivity of YbAu_2Si_2 at various pressures. The data can be described by a phonon scattering model. Figure taken from **B3**.

Besides Yb, Eu is another element among the rare-earths with possibility of valence instability. In the work (**B4**) we have investigated magnetic behavior of EuRu_2P_2 single crystal as a function of pressure. EuRu_2P_2 adopts the tetragonal ThCr_2Si_2 -type of structure. Its ferromagnetic state below $T_{\text{C}} = 29$ K exhibits a small magneto-crystalline anisotropy with the crystallographic a -direction as an easy axis. Our measurements of magnetization, AC-susceptibility and electrical resistivity have shown that its magnetism is given by purely Eu^{2+} atoms. Application of hydrostatic pressure in this case leads to a moderate increase of T_{C} up to 1.5 GPa, followed by its sudden drop by 10 K (Fig. B2,B3). This effect was ascribed to a structure property, namely change in the bulk modulus, reported earlier [23] at room

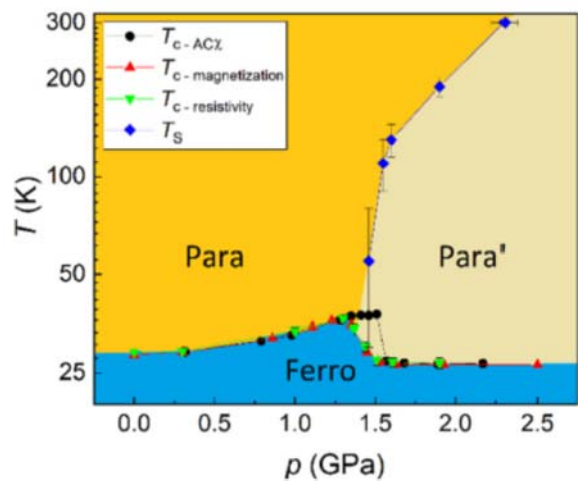


Fig. B2: Temperature – pressure phase diagram of EuRu_2P_2 connecting the pressure evolution of the Curie temperature and the estimated structure anomaly joining at the same T - p point at about (37 K - 1.5 GPa). Figure taken from **B4**.



temperature. Within our study, we followed this anomalous lattice effect down to low temperatures. The critical pressure decreases with decreasing T and reaches 1.5 GPa at low temperatures, where the T_C drops suddenly (see Fig. B2). The drop has been ascribed to a change in exchange interactions. A valence transition cannot be excluded, as well, in case of Eu-based systems. Both these effects may originate in the changes of crystal structure – exchange interaction in rare-earths is generally driven by the RKKY interaction, which depends on rare-earth ionic distances.

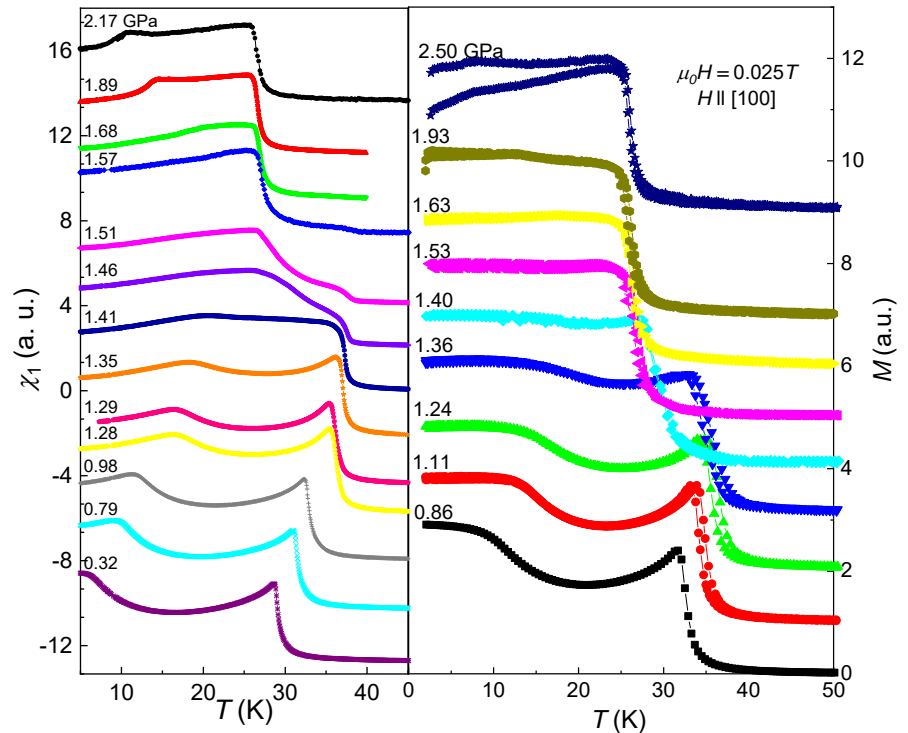


Fig. B3: Temperature dependence of AC magnetic susceptibility – real part (left) and magnetization in a small magnetic field (right) measured at various pressures with fine pressure steps around 1.5 GPa. Figure taken from B4.

On the other hand, the valence state influences the resulting atomic radius – or rather the extent of electron wave functions, so the changes in the valence state are connected with impact on the structure of the material. The decision about the real origin should be answered by the spectroscopic measurements under pressure.

C: Pari-magnetism in $R\text{Co}_2$ under pressure

The family of Laves-phase $R\text{Co}_2$ compounds (R = rare-earth) is known for long time and studied for the specific physical properties, namely their magnetism originating in two different magnetic sublattices. It was deduced that their magnetic properties depend predominantly on the R atoms. Their ordering results in magnetic exchange able to split the Co $3d$ -subbands and form the Co magnetism. As the Co $3d$ band states appear near the critical conditions for the magnetic moment formation, the magnetic properties are very sensitive to external variables and represent a great example for study of itinerant magnetism in Co-contained compounds. The type of transition at the critical temperature is in several cases characterized as the first-order type. Our interest in these compounds was motivated by a discovery of a peculiar phenomenon of short-range magnetic order within the paramagnetic state, denoted as “parimagnetism” [24]. This state represents

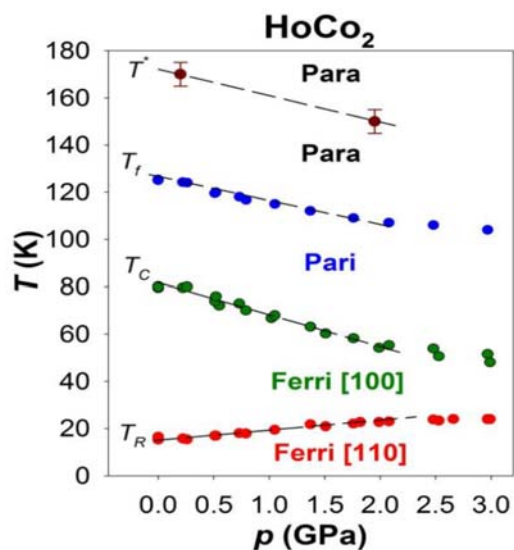


Fig. C1: Pressure evolution of the characteristic temperatures in HoCo_2 – temperature of magnetic moments reorientation T_R , the Curie temperature T_C , the flipping temperature T_f and T^* characterizing presence of the parimagnetic configuration. Figure taken from **C1**.

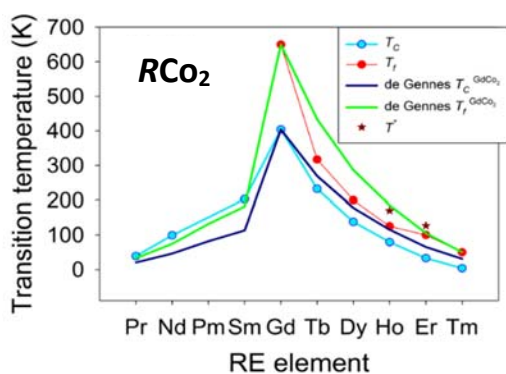


Fig. C2: Estimated temperatures T_C , T_f and T^* for various RCo_2 compounds together with the evolution of the de Gennes factor related to either $T_C^{\text{GdCo}_2}$ or $T_f^{\text{GdCo}_2}$ (dark blue or green line, respectively). T^* marks the onset of the Co-magnetic clusters estimated by the μSR experiment. Data for $R = \text{Pr}, \text{Nd}, \text{Sm}$ [26] and Tb [26,27] are taken from the respective references.

ordering of Co magnetic moments on short distance forming clusters with resulting magnetization antiparallel to the magnetic moment of the rare-earth one. The size of the clusters is quite small – only few elementary-cell units - detectable as a tiny anomaly on the AC-magnetic susceptibility. Another method suitable for detection of this phenomenon was a μSR spectroscopy, which is able to detect presence and changes in the magnetic field inside the lattice of the compound on the local level. Temperature of appearance of the first signal of the new local magnetic field formed by the Co-clusters formation is denoted as T^* . We have used these two methods to study the pressure development of the magnetism in HoCo_2 including parimagnetism in work **C1**. The pressure evolution of the characteristic temperatures is depicted on the Fig. C1. Particularly interesting is the flipping temperature $T_f = 125$ K (characterizing the parimagnetic state) and $T_C = 79.5$ K (ambient pressure) evolving with the same pressure rate signifying similarity in mechanisms responsible for the short and long-range ordering in this system. The reason for the decreasing of T_C with pressure is probably due to the broadening of the Co-3d bands resulting in decrease of the Co magnetic moments and suppression of the Co magnetism and the ordering temperature [25]. On the level of Co clusters the Co-Co distances are decreasing with increasing pressure leading to a broadening of the 3d band and decreasing of the density of states at E_F . Nevertheless the unusually rapid decrease of T_C with pressure is systematically dependent on the rare-earth atom, as studied for several other RCo_2 compounds (**C2,C3**). The summary of the pressure evolution of parimagnetic configuration is included in the publication **C4**. Thanks to numerous studied RCo_2 compounds (by ourselves or found in literature) we could identify several notable systematic dependences. The T_C and T_f

evolution with respect to the included rare earth agrees to a considerable degree with the de-Gennes scaling (Fig. C2). This scaling shows expected variations of magnetic interactions if interactions constants are invariable and the dependence on the type of R is reflecting the appropriate filling of the 4f shell and related quantum numbers. Fig. C2 shows that for heavy R

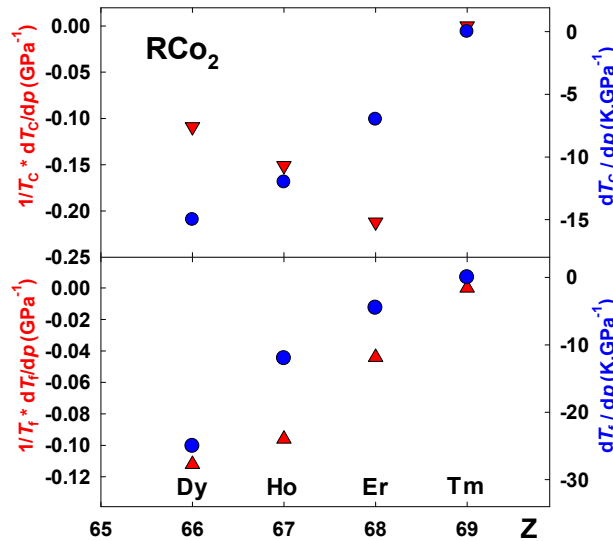


Fig. C3: Systematic evolution of the pressure ratio of T_C (upper part) and T_f (lower part) with the rare-earth element R in $R\text{Co}_2$. Figure taken from C4.

atoms, starting from Gd, it is the paramagnetic flipping temperature T_f which reflects the strength of interactions, while for light R atoms, where the paramagnetic effects are absent, the interaction strength gives directly the T_C values.

The pressure ratio of T_C (T_f) exhibits a systematic rare-earth-element dependence (Fig. C3) with an exceptional case of TmCo_2 (C5). The resulting

findings lead to a volume-dependent relation between T_C and T_f which agrees with the pressure influence (lattice parameters decrease) and the lanthanide contraction (Fig. C4). This empirical systematic dependence is not followed only in the case of substitution of Si for Co (C3) exhibiting a disturbance of the Co-tetrahedron and thus affecting the Co-Co interaction. The paramagnetic temperature T_f is decreasing whereas the ordering temperature T_C increases upon Co-Si substitution. Increase of T_C is probably caused by the increased Co moment (empirically confirmed [28]) while the T_f decrease is given by the disturbance of the Co magnetic clusters by a nonmagnetic Si. The effect of paramagnetism remains a unique configuration on the border between paramagnetism and long-range magnetic order observed in compounds with presence of localized and itinerant magnetism, so far exclusively in the family of $R\text{Co}_2$.

The effect of paramagnetism is thus signal of presence of the magnetic interactions with a potential to create magnetic order which is not strong enough to form the magnetic ordering on the long-scale and thus only formation of the magnetic clusters as precursors of the long-range magnetic order can be observed.

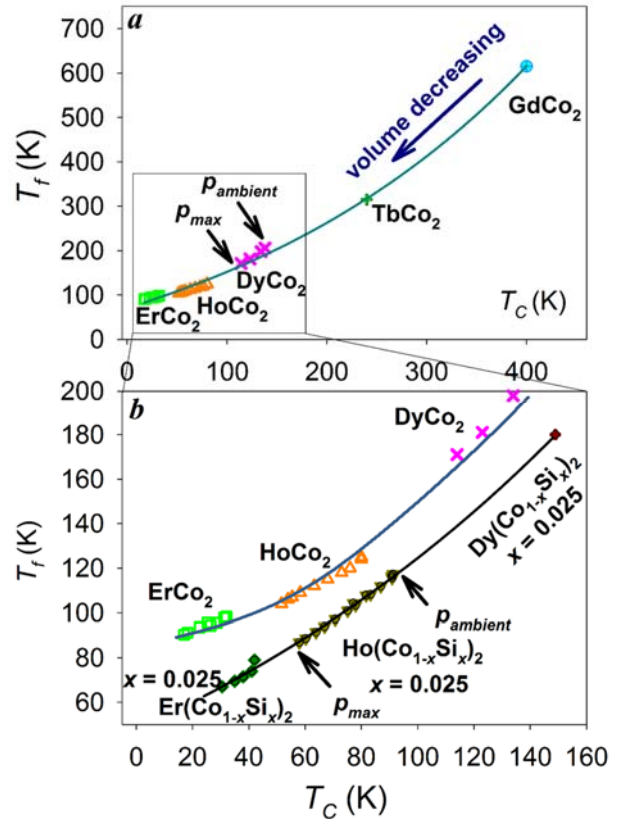


Fig. C4: Relation between the characteristic temperatures T_C and T_f for $R\text{Co}_2$ compounds (a) with $R = (\text{Er}, \text{Ho}, \text{Dy}, \text{Tb}, \text{Gd})$; (b) the detail of the T_f versus T_C dependence of the substituted compounds $R(\text{Co}_{1-x}\text{Si}_x)_2$ where $R = (\text{Er}, \text{Ho}, \text{Dy})$. The lines are to guide the eye.



D: Pressure impact on properties in U and Ce-based compounds

Although the inter-actinide spacing can tune the parameters of the 5f states in uranium systems to a large extent, their full localization is rather exceptional. Among binaries, the only attested 5f localized case is UPd₃, which exhibits a quadrupolar ordering at low temperatures [29,30]. It crystallizes in the hexagonal closed-packed crystal structures with lattice parameters $a = 5.73 \text{ \AA}$ and $c = 9.66 \text{ \AA}$. There are two inequivalent uranium sites in the structure. The distance

between uranium atoms is 4.11 \AA , which is larger than the Hill limit (around $3.4\text{-}3.6 \text{ \AA}$). The pressure application should eventually lead to a delocalization of the 5f states. Such delocalization is often connected with change of bonding conditions, atomic volume and possibly also structural type change. Theoretical electronic structure calculations predicted the delocalization of one 5f electron in pressures about 25 GPa [31]. The system should become a heavy fermion above this pressure. This compound was formerly studied by XRD under pressure [32] and there was found no structural transition or anomaly which could be associated with the delocalization of the 5f states. There was nevertheless still an option of rather smooth delocalization change and the high pressure should affect the resistivity even if there is no structural change. Nevertheless, the delocalization should be a result of high pressure action. In order to prove this fact the high pressure resistivity experiment was performed – **D1**.

The Bridgman anvil pressure cell was used for the measurement on the single crystal of UPd₃ up to 10 GPa. The diameter of the sample space was 1 mm (Fig. D1) and a superconducting transition of Pb was used for the pressure determination. The obtained temperature dependences of resistivity exhibit anomalies below 50 K (Fig. D2), attributed to crystal-field effects [33]. The pressure variations of the measured curve are very small.

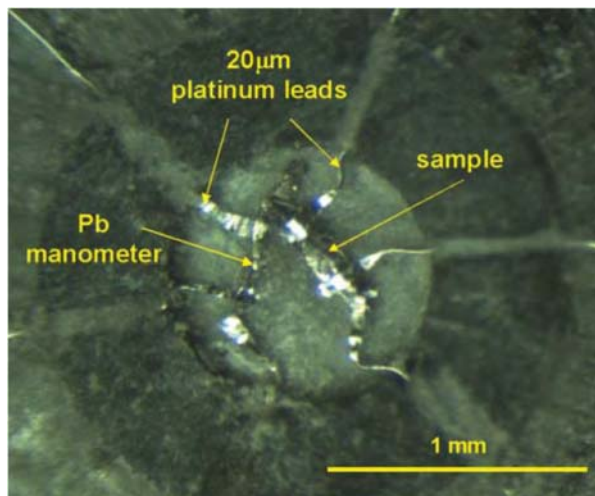


Fig. D1: A microscopic view of the experimental setup just before closing between the two Bridgman anvils.

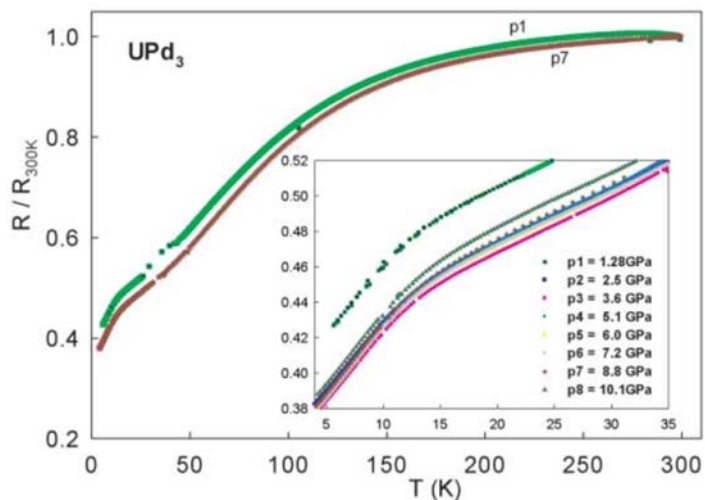


Fig. D2: Temperature dependence of resistance of the UPd₃ compound in various values of pressure. The shift of the data for the lowest pressure about 1.3 GPa is caused by the loose electrical contacts to the sample or the lead inside the cell. This artifact does not appear at higher pressures any more. Figure taken from the publication **D1**.



The detailed analysis based on the second derivative is showing only a very weak shift of the anomaly between 10 and 15 K to higher temperatures (Fig. D3). This can be explained as a small increase in the crystal field splitting. Concerning the signs of delocalization which was expected upon the pressure application, the CEF anomalies should not be present in the delocalized system. Moreover the character would be affected by the spin-fluctuations in case of delocalization, as observed in UPt_3 , which can be used as analogy to UPd_3 with delocalized $5f$ states [34]. As a result, no signal of delocalization was observed up to 10 GPa although the volume was compressed by 4% at the highest pressure. Higher pressures are thus needed for such dramatic effect like $5f$ states delocalization in UPd_3 .

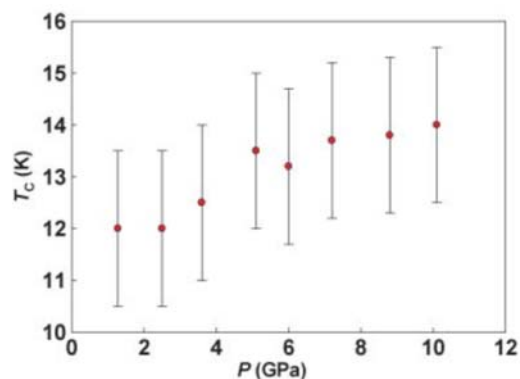


Fig. D3: Pressure variation of temperature of the crystal-field anomaly observed in the resistivity data. Figure taken from **D1**.

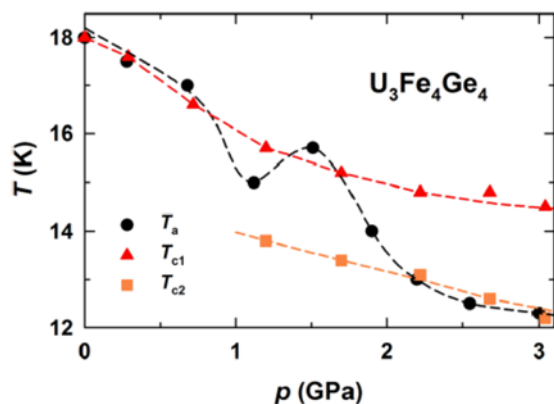


Fig. D4: Pressure dependence of T_a and $T_{c1,2}$ estimated from the measurements of electrical resistivity of $\text{U}_3\text{Fe}_4\text{Ge}_4$ along the a and c axes, respectively. Figure taken from **D2**.

Among numerous uranium-based compounds also $\text{U}_3\text{Fe}_4\text{Ge}_4$ has been studied – with focus on the pressure-induced effects in **D2**. $\text{U}_3\text{Fe}_4\text{Ge}_4$ adopts the orthorhombic crystal structure (space group $Immm$) with two different uranium Wyckoff sites. It orders ferromagnetically below $T_C = 18$ K [35]. Application of pressure leads to a decrease of the Curie temperature, being a fingerprint of itinerant $5f$ states (Fig. D4). At around $p = 1$ GPa the ground state changes from ferromagnetic to antiferromagnetic. At the same pressure also the elastic properties of the crystal lattice change – the direction b changes from the least compressible to the most compressible one.

Based on the measured resistivity data it was found that above the pressure of 1 GPa the system has a tendency to a more isotropic state with increasing pressure, weakly correlated moments along crystallographic a axis or strongly damped magnetic excitations with a wave vector along a . At the pressure of 1 GPa sign of another magnetic ordering are visible for current applied along c -axis at $T_{c2} < T_{c1}$. The pressure-induced changes in magnetic behavior are thus of complex character and connected with change in the elasticity of the crystal lattice, proving an intimate connection between the $5f$ magnetism and crystal lattice.

UH_3 is another representative among the uranium compounds. It forms in two cubic variants – the transient α - UH_3 and the stable β - UH_3 . The $5f$ magnetic moments exhibit ferromagnetic order in β - UH_3 with the Curie temperature reported in the range of 160-170 K [36]. Together with the U-U spacing of some U atoms about 3.3 Å, i.e. below the Hill limit (3.4-3.6 Å), these properties make



this compound rather out of known systematics, showing magnetism appearing usually for compounds with the U-U spacing above the Hill limit.

Existing experimental data on this system were limited due to its pyrophoricity, preventing using common experimental procedures. Hence the peculiar non-linear pressure dependence of T_C obtained by Andreev et al. [37] rose certain suspicions about intrinsic origin of the observed data (Fig. D5). Availability of samples stabilized by a small amount of transition metal with similar T_C and magnetic moment per U enabled to carry out a broader pressure study. Our results (D3) show a slower linear decrease of T_C with pressure. On Fig. D6

we depict the pressure dependence of the maximum and of the inflection point which we estimate as the ordering temperature T_C . The determined pressure dependence is estimated as $dT_C/dp = -1.87$ K/GPa and thus $d \ln T_C/dp = 1/T_C * dT_C/dp = -0.011$ GPa⁻¹. This value is more than twice smaller (in absolute value) than the value of -0.024 GPa⁻¹ reported earlier [37] where it was explained as a sign of the itinerant character of β -UH₃. The much weaker pressure dependence points to more localized character than expected before.

If we take into account the compounds with cubic crystal structure (NaCl-type) with similar compressibility, then we count on UN (band antiferromagnet [38,39]), US (with higher T_C than UH₃ [40]) and UAs (where T_N increases with pressure [41]) from this one can deduce that the 5f character shifts towards localization. Another aspect is the U-U distance in these compounds – which are 3.87 Å (for US), 4.07 Å (for UAs) and 3.45 Å (for UN) – in contrast with the value of 3.31 Å for β -UH₃, it points that UH₃ reaches such degree of localization at much shorter U-U distance. This non-typical behavior is explained by the interaction U-H with 6d-1s hybridization which reduces the 5f-6d hybridization. This fact was stated before in [42] where the influence of H content on the ordering temperature clearly demonstrates higher localization for uranium hydride with higher H content.

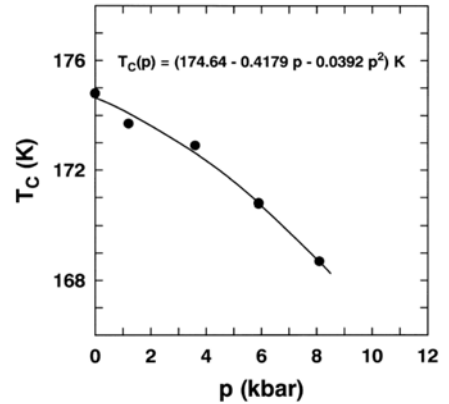


Fig. D5: Pressure dependence of Curie temperature in UH₃ according to [37].

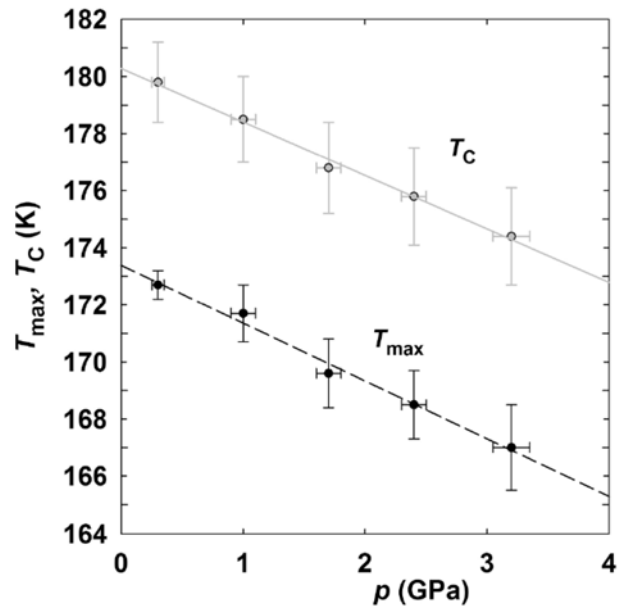


Fig. D6: Pressure dependence of Curie temperature and T_{max} in UH₃ as estimated from the high-pressure AC-susceptibility measurement. Figure taken from D3.



Another uranium based compound studied under pressure is U_2Ni_2Sn – tetragonal compound with a highly anisotropic crystal structure. It is characteristic by two types of basal planes of which one is formed by the U elements alternating with another Ni-Sn planes. It orders antiferromagnetically below $T_N = 25$ K. As shown in **D4**, upon pressure application, the Néel temperature increases up to 3 GPa with a pressure ratio $dT_N/dp = 0.6$ K/GPa. As it appears in many U systems, the U-U distance is the most compressible one, leading to decreasing of the inter uranium distances with increasing pressure. The increase of T_N is a consequence of shrinking the basal plane and thus increasing overlap of the $5f$ wavefunctions. At the pressure of 3 GPa the ordering temperature suddenly changes its pressure evolution by a different slope and a sharp decrease (Fig. D7). As it was found by a high pressure structural study, this sudden downturn is connected with a change of the crystal lattice symmetry to orthorhombic structure type. As confirmed by theoretical calculations, the collapse of magnetism above 3 GPa is given by the pressure-driven decreasing of U-U distances resulting in broadening of the $5f$ shell and decreasing of density of states at the Fermi level. From the obtained results it is clear that the special type of U crystallographic arrangement and tunability of the inter-uranium distances plays an important role in the magnetic properties of compounds adopting this type of structure.

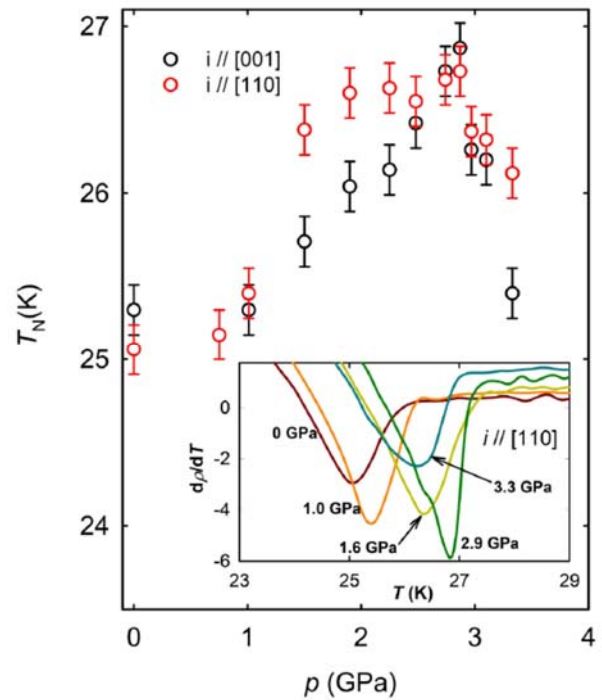
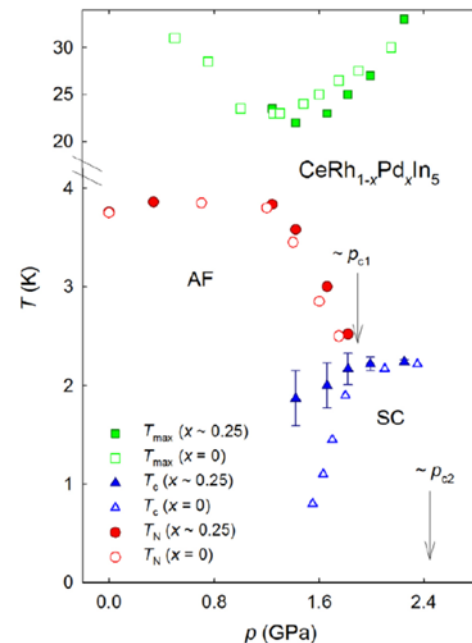


Fig. D7: Pressure dependence of the Néel temperature of U_2Ni_2Sn derived from the zero-field resistivity. The inset shows the temperature dependence of the $d\rho/dT$ derivatives at the selected pressures for $i//[110]$ in the vicinity of the ordering temperature of U_2Ni_2Sn . The minima on these derivatives have been used for tracking the $T_N(p)$ dependence. Figure taken from the publication **D4**.



A close relationship between superconductivity and magnetism with signs of quantum criticality has been studied on two Cerium compounds CeRhSi_3 and CeRhIn_5 . CeRhIn_5 adopts the tetragonal structure with a possible view of a quasi-2D structure of RhIn_2 layers alternating with CeIn_3 layers along the c -axis. This compound belongs to heavy-fermion systems ordering antiferromagnetically below $T_N = 3.8$ K. The ground-state magnetic structure is incommensurate with helicoidally arranged moments within the basal plane [43]. Upon magnetic field application another field-induced transitions at T_1 and T_2 appear below T_N . A frustration between nearest-neighbor and next-nearest-neighbor magnetic moments along the c -axis stands behind a complex magnetic behavior [44]. Application of a pressure induces a superconductivity coexisting with the antiferromagnetic order up to pressure of about 2 GPa. Only the superconductivity is present above this pressure [45].

In the work **D5**, a substitution Pd instead of Rh was applied. The resistivity measurements of the substituted $\text{CeRh}_{0.75}\text{Pd}_{0.25}\text{In}_5$ single crystal have shown a maximum above T_N for hydrostatic pressures above 1 GPa – similar to the parent CeRhIn_5 . The established temperature-pressure phase diagram (Fig. D8) reveals only a negligible difference of the magnetic-phase-transition temperatures of the substituted compound from the pristine one. On the other hand, the superconductivity sets at markedly lower pressures in the Pd-doped compound exhibiting the Pd-Rh substitution as a tool shifting the coexistence of magnetism and superconductivity in the $\text{CeRh}_{1-x}\text{Pd}_x\text{In}_5$ system closer to the ambient pressure.



*Fig. D8: Phase diagram of $\text{CeRh}_{1-x}\text{Pd}_x\text{In}_5$ with $x = 0$ and $x = 0.25$ comparing the pressure dependence of the magnetic (T_N , T_{\max}) and superconducting (T_c) properties. Values for pure CeRhIn_5 were taken from Refs. [45,46]. Figure taken from **D5**.*



In the case of a tetragonal non-centrosymmetric CeRhSi_3 a superconducting transition T_c was reported to appear at the pressure of 0.4 GPa inside the antiferromagnetic phase, which exists below $T_N = 1.6$ K at ambient pressure. The pressure dependence of T_N forms a broad maximum until it merges with the superconducting transition T_c at the pressure of 2.4 GPa and temperature of 1.1 K (Fig. D9). The Ce magnetic moments have been characterized as itinerant over the whole pressure range up to 3 GPa [47]. Later studies tracked the superconductivity borderline to higher pressures [48], showing the superconducting dome ending at about 5 GPa. The presence of superconductivity hiding many details of magnetism did not allow to investigate the possible quantum critical point at low temperatures.

In the paper **D6** we used a substitution of Ge instead of Si in CeRhSi_3 in order to shift and possibly separate the antiferromagnetic phase from the superconducting one. The substitution leads to an expansion of the lattice in accordance with the Si-Ge size effect, resulting into an enhancement of magnetism (increasing T_N with substitution ratio) and shift of the onset of superconductivity to higher pressures – see Fig. D10. The development of T_N and T_c supports the idea of a quantum critical point (QCP) present inside the superconducting dome for the substituted compounds and presumably also in the pristine CeRhSi_3 .

In summary, to compare the effect of pressure application on intermetallic systems based on rare-earth, especially the cerium, or uranium, one can see that the pressure is a very powerful tool for tuning their physical properties. The key property is pressure-driven change of the crystal lattice, namely the interatomic distances of the magnetic ions which influences both – interactions (major issue in the case of the localized magnetic moments like rare-earth intermetallic compounds) and conditions for magnetic moment formation which is

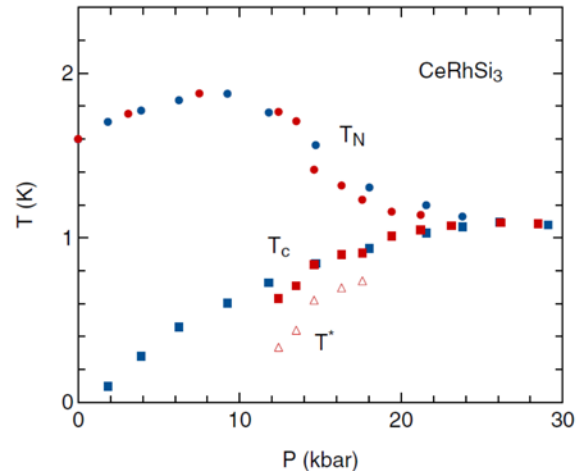


Fig. D9: Néel temperature T_N merging with the superconducting temperature T_c in pure CeRhSi_3 – figure taken from [49].

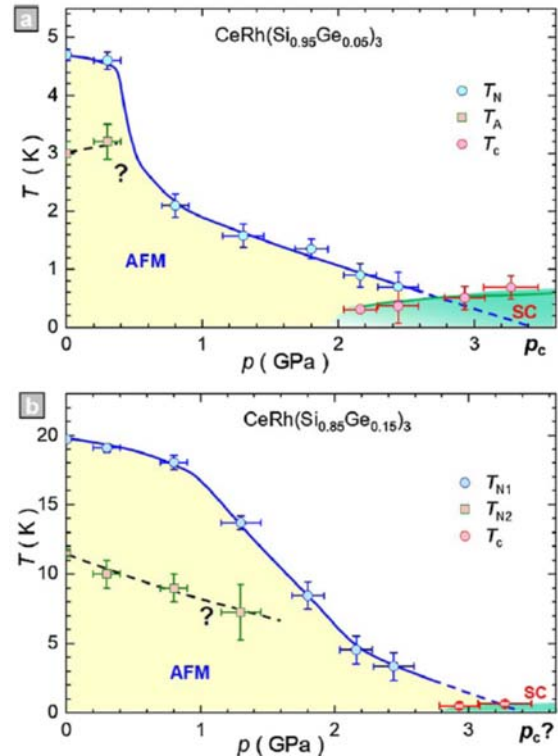


Fig. D10: Néel temperature T_N merging with the superconducting temperature T_c in higher pressures upon higher substitution ratio ($x=0.05$ upper part, $x=0.15$ lower part). Figure taken from **D6**.



significant in the case of itinerant systems (uranium- and very often cerium based compounds, 3d metals). External pressure forces the system towards a lower volume configuration and uncovers the preferred ground state of the studied system upon changed volume by the most pure way – i.e. by direct mechanical influence of the crystal lattice. A special case form compounds with potential to valence changes due to different atomic extent of different valence configurations. Knowledge of the structural aspects of the intermetallic compounds are thus very important for resolving of the background of their changed behavior upon varied external conditions from which the pressure influence on several systems is presented in this overview.

References:

- [1] N.W. Ashcroft, N.D. Mermin: *Solid State Physics*, Saunders College, Philadelphia, 1976
- [2] Ch. Kittel: *Úvod do fyziky pevných látek*, Academia, Praha, 1985
- [3] M. Eremets, *High Pressure Experimental Methods*, Oxford University Press Inc., New York, 1996
- [4] W.F. Sherman and A.A. Stadtmuller, *Experimental Techniques in High-Pressure Research*, John Wiley & Sons Ltd., Chichester, 1987
- [5] S. Klotz, *Techniques in High Pressure Neutron Scattering*, CRC press (Taylor & Francis), London, 2013
- [6] K. Yokogawa, K. Murata, H. Yoshino, S. Aoyama, *Japanese Journal of Applied Physics* **46** (2007) 3636.
- [7] K. Murata, K. Yokogawa, H. Yoshino, S. Klotz, P. Munsch, A. Irizawa, M. Nishiyama, K. Iizuka, T. Nanba, T. Okada, Y. Shiraga, S. Aoyama, *Review of Scientific Instruments* **79** (2008) 085101.
- [8] K. Murata, S. Aoki, *Review of High Pressure Science and Technology* **26** (2016) 3.
- [9] Idemitsu Kosan Co. Ltd.; Daphne Oil 7575 Data sheet
- [10] G. Ehlers, *Frustrierte magnetische 4f-Momente in intermetallischen Verbindungen der Lanthaniden, die in der ZrNiAl-Struktur kristallisieren*, Ph.D. thesis, Berlin, 1997.
- [11] F. Merlo, S. Cirafici, F. Canepa, *Journal of Alloys and Compounds* **266** (1998) 22.
- [12] J. Jarosz, E. Talik, T. Mydlarz, J. Kusz, H. Böhm, A. Winiarski, *Journal of Magnetism and Magnetic Materials* **208** (2000) 169.
- [13] E. Talik, M. Skutecka, J. Kusz, H. Böhm, J. Jarosz, T. Mydlarz, A. Winiarski, *Journal of Alloys and Compounds* **325** (2001) 42.
- [14] L. Havela, M. Diviš, V. Sechovský, A.V. Andreev, F. Honda, G. Oomi, Y. Méresse, S. Heathman, *Journal of Alloys and Compounds* **322** (2001) 7.
- [15] M. Klicpera, P. Javorský, A. Hoser, *Journal of Alloys and Compounds* **596** (2014) 167.
- [16] L.C. Chapon, E.A. Goremychkin, R. Osborn, B.D. Rainford, S. Short, *Physica B* **378-380** (2006) 819.
- [17] M. Klicpera, M. Boehm, P. Doležal, H. Mutka, M.M. Koza, S. Rols, D.T. Adroja, I. Puente Orench, J. Rodríguez-Carvajal, P. Javorský, *Physical Review B* **95** (2017) 085107.
- [18] J. Kitagawa, M. Ishikawa, *Journal of the Physical Society of Japan* **68** (1999) 2380.
- [19] P. Doležal, D. Kriegner, M. Klicpera, M. Diviš, J. Prchal, Z. Mičková, P. Javorský, *Journal of Alloys and Compounds* **790** (2019) 480.
- [20] T. Shigeoka, N. Iwata, H. Fujii, *Journal of Magnetism and Magnetic Materials* **104-107** (1992) 1229.
- [21] S. Watanabe, K. Miyake, *Physical Review Letters* **105** (2010) 186403.
- [22] Z. Ren, L.V. Pourovskii, G. Girit, G. Lapertot, A. Georges, D. Jaccard, *Physical Review X* **4** (2014) 031055.
- [23] C. Huhnt, W. Schlabit, A. Würth, A. Mewis, M. Reehuis, *Physica B* **252** (1998) 44.
- [24] J. Herrero-Albillos, F. Bartolomé, L. M. García, A. T. Young, T. Funk, J. Campo, G. J. Cuello, *Physical Review B*, **76** (2007) 094409.



- [25] O. Syshchenko, T. Fujita, V. Sechovský, M. Diviš, H. Fujii, *Journal of Alloys and Compounds* **317** (2001) 438.
- [26] R. Hauser, E. Bauer, E. Gratz, *Physical Review B* **57** (1998) 2904.
- [27] J. Herrero-Albillos, private communication; C.M. Bonilla, oral contribution on 56th MMM conference
- [28] T.D. Cuong, *Magnetism and related properties of RECo₂ compounds: Co-dilution*, Ph.D. thesis, Prague, 1998.
- [29] Y. Baer, H.R. Ott, K. Andres, *Solid State Communications* **36** (1980) 387.
- [30] K.A. McEwen, H.C. Walker, M.D. Le, D.F. McMorrow, E. Colineau, F. Wastin, S.B. Wilkins, J.-G. Park, R.I. Bewley, D. Fort, *Journal of Magnetism and Magnetic Materials* **310** (2007) 718.
- [31] L. Petit, A. Svane, W. M. Temmerman, Z. Szotek, *Physical Review Letters* **88** (2002) 216403.
- [32] S. Heathman, M. Idiri, J. Rebizant, P. Boulet, P. S. Normile, L. Havela, V. Sechovský, T. Le Bihan, *Physical Review B* **67** (2003) 180101.
- [33] P. Zaplinski, D. Meschede, D. Plumacher, W. Schlabit, H. Schneider, in *Proceedings of the International Conference on Crystalline Electric Field and Structural Effects in f-Electron Systems*, New York (1980) 295.
- [34] A. de Visser, J.J.M. Franse, A. Menovsky, *Journal of Magnetism and Magnetic Materials* **43** (1984) 43.
- [35] M.S. Henriques, D.I. Gorbunov, J.C. Waerenborgh, L. Havela, A.V. Andreev, Y. Skourski, A.P. Gonçalves, *Journal of Alloys and Compounds* **555** (2013) 304.
- [36] R. Troc, W. Suski, *Journal of Alloys and Compounds* **219** (1995) 1.
- [37] A.V. Andreev, S.M. Zadvorkin, M.I. Bartashevich, T. Goto, J. Kamarád, Z. Arnold, H. Drulis, *Journal of Alloys and Compounds* **267** (1998) 32.
- [38] J.M. Fournier, J. Beille, C.H. de Novion, *Journal de Physique Colloque* **40** (1979) C4-32.
- [39] J. Staun Olsen, L. Gerward, U. Benedict, *Journal of Applied Crystallography* **18** (1985) 37.
- [40] C.Y. Huang, R.J. Laskowski, C.E. Olsen, J.L. Smith, *Journal de Physique Colloque* **40** (1979) C4-26.
- [41] I.N. Goncharenko, J.-M. Mignot, V.A. Somenkov, J. Rossat-Mignod, O. Vogt, *Physica B* **199&200** (1994) 625.
- [42] L. Havela, M. Paukov, M. Dopita, L. Horák, D. Drozdenko, M. Diviš, I. Turek, D. Legut, L. Kyvala, T. Gouder, A. Seibert, F. Huber, *Inorganic Chemistry* **57** (2018) 14272.
- [43] S. Raymond, E. Ressouche, G. Knebel, D. Aoki, J. Flouquet, *Journal of Physics: Condensed Matter* **19** (2007) 242204.
- [44] P. Das, S.-Z. Lin, N.J. Ghimire, K. Huang, F. Ronning, E.D. Bauer, J.D. Thompson, C.D. Batista, G. Ehlers, M. Janoschek, *Physical Review Letters* **113** (2014) 246403.
- [45] G. Knebel, D. Aoki, J.P. Brison, L. Howald, G. Lapertot, J. Panarin, S. Raymond, J. Flouquet, *Physica Status Solidi b* **247** (2010) 557.
- [46] T. Park, Y. Tokiwa, F. Ronning, H. Lee, E.D. Bauer, R. Movshovich, J.D. Thompson, *Physica Status Solidi b* **247** (2010) 553.
- [47] T. Terashima, Y. Takahide, T. Matsumoto, S. Uji, N. Kimura, H. Aoki, H. Harima, *Physical Review B* **76** (2007) 054506.
- [48] D. Staško, J. Valenta, M. Kratochvílová, J. Prchal, P. Prosczek, M. Klicpera, *Journal of Physics: Condensed Matter* **33** (2021) 035602.
- [49] N. Kimura, Y. Muro, H. Aoki, *Journal of the Physical Society of Japan* **76** (2007) 051010.



List of attached publications

T - Technical (pressure transmitting media characterization)

T1) D. Staško, [J. Prchal](#), M. Klicpera, S. Aoki, K. Murata, **Pressure media for high pressure experiments, Daphne Oil 7000 series**, High Pressure Research, **40**, Issue 4, 2020, 525-536. (DOI: 10.1080/08957959.2020.1825706)

① Results/publication participation: Whole work performed by D.Staško under supervision of Jiří Prchal (J.P.) in frame of a Students project in CU FMP. Publication with help of other coauthors.

A - Structural changes in magnetics under pressure

A1) [J. Prchal](#), P. Javorský, J. Ruzs, F. de Boer, M. Diviš, H. Kitazawa, A. Dönni, S. Daniš, V. Sechovský, **Structural discontinuity in the hexagonal RTAl compounds: Experiments and density-functional theory calculations**, Physical Review B, **77**, No.13, 2008, 134106. (DOI: 10.1103/PhysRevB.77.134106)

① Results/publication participation: Most of the structural study (low-temperature- and composition dependence) on the presented compounds, author of the idea of forbidden c/a values in this crystal structure type. Manuscript preparation (and other results including theoretical calculations) with help of other coauthors.

A2) [J. Prchal](#), M. Klicpera, P. Doležal, J. Kaštil, M. Mišek, P. Javorský, **Pressure effect on the isostructural transition in RNiAl compounds ($R=Tb$ and Gd)**, Journal of Physics: Conference Series, **500**, 2014, 032013. (DOI: 10.1088/1742-6596/500/3/032013)

① Results/publication participation: Measurements of resistivity under pressure performed under supervision of J.P. mainly in frame of Bc thesis (P.Doležal) and practical part of the lecture High pressure physics (M.Klicpera) in FMP CU under supervision of J.P. Publication with support of other coauthors.

A3) J. Kaštil, M. Klicpera, [J. Prchal](#), M. Mišek, J. Prokleška, P. Javorský, **Effect of hydrostatic and uniaxial pressure on structural and magnetic transitions in TbNiAl**, Journal of Alloys and Compounds, **585**, 2014, 98-102. (DOI: 10.1016/j.jallcom.2013.09.129)

① Results/publication participation: Participation on the hydrostatic-pressure experiment.

A4) P. Javorský, [J. Prchal](#), M. Klicpera, J. Kaštil, M. Mišek, **Pressure Influence on Magnetic Properties of TbNiAl**, Acta Physica Polonica A, **126**, 2014, 280-281. (DOI: 10.12693/APhysPolA.126.280)

① Results/publication participation: Participation on the hydrostatic-pressure experiment.

A5) M. Klicpera, P. Doležal, J. Prokleška, [J. Prchal](#), P. Javorský, **Magnetic and transport properties of CePd₂Al₂ single crystal**, Journal of Alloys and Compounds, **639**, 2015, 51-59. (DOI: 10.1016/j.jallcom.2015.03.095)

① Results/publication participation: Data of resistivity under pressure obtained within diploma thesis of P.Doležal supervised by J.P. Publication with support of other coauthors.

A6) P. Doležal, M. Klicpera, [J. Prchal](#), P. Javorský, **Structural phase transition in CePd₂Ga₂ under hydrostatic pressure**, Acta Physica Polonica A, **127**, 2015, 219-221. (DOI: 10.12693/APhysPolA.127.219)

① Results/publication participation: Data of resistivity under pressure obtained within diploma thesis of P.Doležal supervised by J.P. Publication with support of other coauthors.



B - Magnetism in rare-earth based RT_2X_2 tetragonal compounds influenced by pressure

- B1)** J. Vejpravová, J. Kamarád, [J. Prchal](#), J. Prokleška and V. Sechovský, ***Magnetic and transport Properties of $PrRu_2Si_2$ Single Crystal Under High Pressure***, Journal of the Physical Society of Japan, **76**, 2007, 49-50. (DOI: 10.1143/jpsj.76sa.49)
① ***Results/publication participation: Participation on the hydrostatic-pressure experiment.***
- B2)** J. Vejpravová, J. Kamarád, [J. Prchal](#), J. Prokleška, V. Sechovský, ***High-pressure effect on magnetic phases in $PrRu_2Si_2$ single crystal***, High Pressure Research, **26** no.4, 2006, 499-502.
① ***Results/publication participation: Participation on the hydrostatic-pressure experiment.***
- B3)** J. Kaštil, M. Míšek, J. Kamarád, Z. Arnold, K. Vlášková, [J. Prchal](#), M. Diviš, P. Doležal, J. Prokleška, J. Valenta, J. Fikáček, A. Rudajevová, D. Kriegner, ***Properties of the divalent-Yb compound $YbAu_2Si_2$ under extreme conditions***, Physica B, **505**, 2017, 41-44. (DOI: 10.1016/j.physb.2016.10.030)
① ***Results/publication participation: Participation on the hydrostatic-pressure experiment and manuscript preparation.***
- B4)** P. Proschek, [J. Prchal](#), M. Diviš, J. Prokleška, K. Vlášková, J. Valenta, J. Zubáč, J. Kaštil, M. Hedo, T. Nakama, Y. Onuki, F. Honda, ***Weakly anisotropic ferromagnet $EuRu_2P_2$: Ambient and hydrostatic pressure characterization***, Journal of Alloys and Compounds, **864**, 2021, 158753 (DOI: 10.1016/j.jallcom.2021.158753)
① ***Results/publication participation: Experimental work performed mainly by students P. Proschek and J. Zubáč in frame of PhD thesis and GAUK project, both supervised by J.P. Publication with help of other coauthors. Manuscript preparation.***

C – Pari-magnetism in RCO_2 : pressure influence

- C1)** J. Valenta, [J. Prchal](#), R. Khasanov, M. Kratochvílová, M. Míšek, M. Vališka, V. Sechovský, ***Presence of paramagnetism in $HoCo_2$ under hydrostatic pressure***, Journal of Physics: Conference Series, **500**, 2014, 182041. (DOI: 10.1088/1742-6596/500/18/182041)
① ***Results/publication participation: Work performed mainly by J.Valenta in frame of his Bc. thesis under supervision of J.P. With partial support of other coauthors.***
- C2)** M. Míšek, J. Prokleška, V. Sechovský, D. Turčinková, [J. Prchal](#), A.F. Kusmartseva, K.V. Kamenev, J. Kamarád, ***Effects of high pressure on the magnetism of $ErCo_2$*** , Journal of Applied Physics, **111**, 2012, 07E132. (DOI: 10.1063/1.3676014)
① ***Results/publication participation: Participation on the hydrostatic-pressure experiment.***
- C3)** J. Valenta, [J. Prchal](#), M. Kratochvílová, M. Míšek, V. Sechovský, ***Presence of Paramagnetism in $Ho(Co_{1-x}Si_x)_2$ Under Hydrostatic Pressure***, Acta Physica Polonica A, **126**, 2014, 406-408. (DOI: 10.12693/APhysPolA.126.406)
① ***Results/publication participation: Work performed mainly by J.Valenta in frame of his master thesis under supervision of J.P. With partial support of other coauthors.***



C4) [J. Prchal](#), J. Šebesta, J. Valenta, M. Míšek, D. Turčinková, L. Lapčák, J. Prokleška, M. Kratochvílová, V. Sechovský, **Magnetism in $R\text{Co}_2$ ($R=\text{Dy, Ho, Er, Tm}$) Under Hydrostatic Pressure**, Acta Physica Polonica A, **126**, 2014, 288-289. (DOI: 10.12693/APhysPolA.126.288)

① *Results/publication participation: Work performed mainly by students J.Šebesta, J.Valenta and L.Lapčák in frame of their Bc. and MSc. theses supervised by J.P. With partial support of other coauthors.*

C5) J. Šebesta, [J. Prchal](#), J. Valenta, M. Kratochvílová, V. Sechovský, **Magnetism in TmCo_2** , Acta Physica Polonica A, **127**, 2015, 379-381. (DOI: 10.12693/APhysPolA.127.379)

① *Results/publication participation: Work performed mainly by J.Šebesta in frame of his master thesis and GAUK project, both supervised by J.P. With partial support of other coauthors.*

D - Pressure impact on properties in U and Ce-based compounds

D1) [J. Prchal](#), L. Havela, A.V. Andreev, **High-pressure resistivity of UPd_3** , High Pressure Research, **32**, 2012, 208-212. (DOI: 10.1080/08957959.2011.649281)

① *Results/publication participation: Performance of the quasi-hydrostatic-pressure experiment (resistivity in BAC cell up to 10 GPa). Manuscript preparation.*

D2) M.S. Henriques, D.I. Gorbunov, A.V. Andreev, [J. Prchal](#), P. Raison, S. Heathman, Z. Arnold, J.-C. Griveau, E. Collineau, L. Havela, A.P. Gonçalves, **Structural and electronic response of $\text{U}_3\text{Fe}_4\text{Ge}_4$ to high pressure**, Journal of Applied Physics, **117**, 2015, 113901. (DOI: 10.1063/1.4914958)

① *Results/publication participation: Participation on the hydrostatic-pressure experiment (el. resistivity).*

D3) [J. Prchal](#), V. Buturlim, J. Valenta, M. Dopita, M. Divis, I. Turek, L. Kyvala, D. Legut, L. Havela, **Pressure variations of the 5f magnetism in UH_3** , Journal of Magnetism and Magnetic Materials, **497**, 2020, 165993. (DOI: 10.1016/j.jmmm.2019.165993)

① *Results/publication participation: Hydrostatic-pressure experiment (AC-magnetic susceptibility). Other experiments and theoretical calculations with help of other coauthors.*

D4) S. Mašková-Černá, A. Kolomiets, [J. Prchal](#), I. Halevy, V. Buturlim, M. Nikolaevsky, O. Koloskova, P. Kozelj, M. König, M. Diviš, L.M. Sandratskii, J. Kaštil, A.V. Andreev, E. Svanidze, L. Havela, **Insight into the physics of the 5f band antiferromagnet $\text{U}_2\text{Ni}_2\text{Sn}$ from the pressure dependence of crystal structure and electrical resistivity**, Physical Review B, **103**, 2021, 035104. (DOI:10.1103/PhysRevB.103.035104)

① *Results/publication participation: High-pressure resistivity experiment performance, participation on the manuscript preparation.*

D5) M. Kratochvílová, K. Uhlířová, [J. Prchal](#), J. Prokleška, M. Míšek, V. Sechovský, **Tuning the pressure-induced superconductivity in Pd-substituted CeRhIn_5** , Journal of Physics: Condensed Matter, **27**, 2015, 095602 (8pp). (DOI: 10.1088/0953-8984/27/9/095602)

① *Results/publication participation: Measurements of resistivity under pressure performed by M. Kratochvílová in frame of the practical part of the lecture High pressure physics in FMP CU under supervision of J.P.*



D6) J. Valenta, T. Naka, M. Diviš, M. Vališka, P. Proschek, K. Vlášková, M. Klicpera, J. Prokleška, J. Custers, [J. Prchal](#), ***Impact of isoelectronic substitution and hydrostatic pressure on the quantum critical properties of CeRhSi₃***, Journal of Physics: Condensed Matter, **32**, 2020, 425601 (DOI: 10.1088/1361-648X/aba015)

① Results/publication participation: *Work on several samples mainly performed by J.Valenta in frame of PhD and GAUK project under supervision of J.P., with partial support of other coauthors.*